

A Theory of the Initial Avalanche in the Breakdown of a Discharge Counter in Helium

SANBORN C. BROWN

Massachusetts Institute of Technology, Cambridge, Massachusetts

(Received July 9, 1942)

On the basis of the discussion on Townsend's criterion for breakdown, definite hypotheses are arrived at as to the behavior of both the positive ions and the photons in the initial avalanche in the breakdown between coaxial cylinders in helium. Calculations of the shape of the field through which the avalanche passes show that to a good approximation the field is proportional to $1/r$ up to a point where the space charge effect of the positive ions in the avalanche starts to modify the field, and thereafter the field through which the avalanche travels can be considered constant. The functional form of the photon effect leads to the assumption that two types of photons are operative, which can be identified with the resonance radiation of He I and He II. Theoretically derived graphical methods for predicting breakdown voltages are given. Comparison between theoretical and experimental threshold curves leads to good agreement for all cylindrical geometries from that usually employed in Geiger-Müller counters up to the limiting case of parallel plates.

A NUMBER of attempts have been made to explain the observed breakdown characteristics of discharge counters, but all of these have dealt only with the special geometrical conditions of the Geiger-Müller counter.¹ The following discussion treats the breakdown characteristics between coaxial cylinders in general up to the limiting case of parallel plates. It deals only with the first avalanche, that is the group of ions and electrons formed by the initial charged particle, and does not treat the action of the succeeding avalanches which build up the space charge which finally quenches the discharge. The experimental data, and therefore the entire discussion, have been carried out only for helium gas contaminated with mercury vapor.

The Townsend criterion for breakdown of a self-maintaining discharge states that

$$\gamma n = 1. \tag{1}$$

γ is the number of electrons liberated at the cathode per ionization in the gas and n is the number of ion pairs formed in the initial discharge. The investigation proceeded in the following manner. First, experimental curves of the threshold voltage for cylinders of various different radii were obtained. Second, the mathematical forms for n and γ were sought which would fit the experimental threshold curves and would be useful in predicting threshold voltages in terms of the counters. Third, a reasonable

physical interpretation was given for these theoretical functions.

EXPERIMENTAL

The experimental curves of threshold voltage as a function of pd are shown in Fig. 1. The

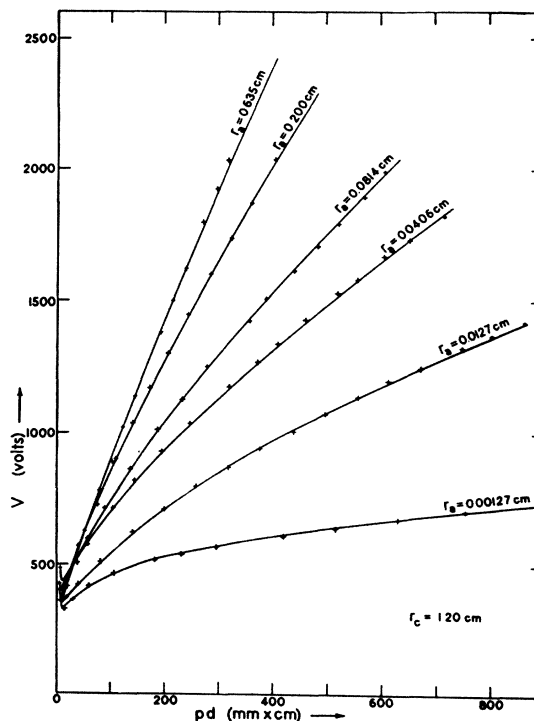


FIG. 1. Threshold voltage for discharge counters of varying anode radius and constant cathode radius for helium contaminated with mercury vapor.

¹ S. Werner, *Zeits. f. Physik* 90, 384 (1934).

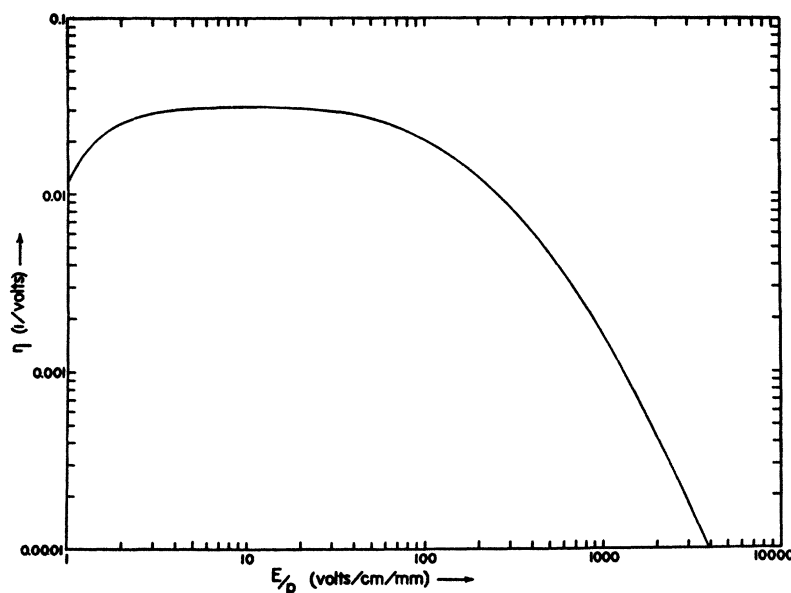


FIG. 2. The ionization per volt as a function of E/p calculated from Engel and Steenbeck's data for helium (contaminated with mercury vapor).

pressure p is measured in mm of mercury. d is the width of the gap between the cathode and the anode and is, therefore, $r_c - r_a$ where r_c and r_a are the radii of the cathode and anode, respectively. The threshold voltage is taken to be that potential for which all pulses from the counting tube due to an external source of radiation are of the same size. This is a sharply defined point and one which marks the lower edge of the discharge counter region in which a self-maintaining discharge occurs in the counter. The gas used was ordinary tank helium and the pressure was measured by means of a mercury manometer. The gas was, therefore, neither of high purity nor free from mercury vapor.

APPLICATION OF THE TOWNSEND THEORY

The Townsend theory tells us in Eq. (1) that to support a self-maintaining discharge, the voltage between the electrodes must be of sufficient magnitude so that the ionization by collision of an entering charged particle is large enough to create enough ion-pairs in the avalanche in order that the photons created in the initial avalanche strike the cathode surface, and produce at least one electron to keep the discharge going.

If α , the first Townsend coefficient, is the

number of ion pairs formed per centimeter of path of the initiating electron as it travels through the field E , it is well known that α/p is a function of E/p where p is the pressure in millimeters of mercury. The form of this function has been measured experimentally many times. It seems more significant, however, from a theoretical point of view, to discuss the problem in terms of a coefficient η , the ionization per volt.² η itself is a function of E/p and is related to α through the equation $\eta = \alpha/E$. The relation between η and E/p , calculated from Engel and Steenbeck's³ curve of α/p as a function of E/p , is shown in Fig. 2. The data of Engel and Steenbeck apply to parallel plates and to helium contaminated with mercury vapor corresponding to that used in the present investigation. The reason for not using pure He is the practical one that counters do not work as satisfactorily with the pure gas. A logical explanation of this can be found in the fact that pure rare gas atoms have high lying metastable levels which have a long enough lifetime to introduce spurious counts in the counter. Even small admixtures of mercury vapor, whose ionization potential is lower than

² M. J. Druyvesteyn and F. M. Penning, *Rev. Mod. Phys.* **12**, 87 (1940).

³ A. Engel and M. Steenbeck, *Elektrische Gasentladungen* (Julius Springer, 1932), p. 105.

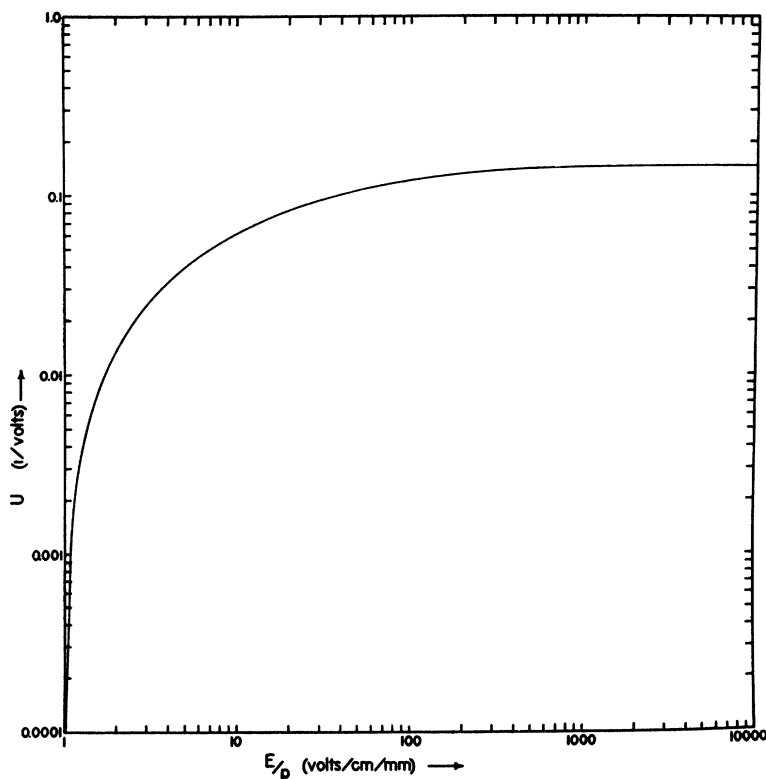


FIG. 3. The function u defined in Eq. (4) is shown plotted against E/p .

the metastable levels in He, will prevent the long life of the metastable states by the ionization of the Hg atoms, and thus prevent the spurious counts which make the pure gas counters unsatisfactory.

One may determine the total number of ion pairs formed in a discharge from the relation that $dn = -\alpha n dr$ and therefore

$$n = \exp \int_{r_c}^{r_a} \alpha dr. \quad (2)$$

For cylindrical geometry α depends on r and the straightforward method of computing n for a particular case would be to plot a curve of α as a function of r for values of the field E computed from the equation

$$E = 2q/r,$$

where

$$2q = V / \ln \frac{r_c}{r_a} \quad (3)$$

and V is plotted in Fig. 1. The curve of α as a

function of r could be graphically integrated to determine n .

This is a very tedious procedure, and to avoid it the following method was introduced. Since $E = 2q/r$ we may write

$$\int -\alpha dr = 2q \int (\alpha/E^2) dE.$$

Actually we would prefer this expression in terms of η and E/p and we therefore have

$$\int -\alpha dr = 2q \int \frac{\eta p}{E} d(E/p).$$

We may therefore define a function u such that

$$u = \int_0^{E/p} \frac{\eta p}{E} d(E/p) \quad (4)$$

and we may rewrite Eq. (2) in the form

$$n = \exp [2q(u_a - u_c)], \quad (5)$$

where u_a refers to the value of u at the anode and u_c its value at the cathode. The usefulness

of this function u comes from the fact that it is a function of E/p alone for a particular gas and can therefore be computed once and for all for this gas. No further integrations need be made in determining n for any cylindrical geometry as long as Eq. (3) holds. Figure 3 shows the form of u , computed from Engel and Steenbeck's data, plotted as a function of E/p .

FORM OF THE INITIAL AVALANCHE

The electric field between two charged coaxial cylinders is proportional to $1/r$. In general if an electron enters the counter at r_c it will first travel in a part of the field which is so low that no ionization by collision takes place. The part of the field in which no ionization takes place will be called the 0 region. In this work we have considered that the 0 region extends to the point where $E/p=1$, E being measured in volts per centimeter and p in millimeters of mercury. For values of E/p greater than 1, ionization by collision takes place, giving rise to the formation of an avalanche. The space in which this occurs is designated as the A region. If one considers that the field remains proportional to $1/r$ from $E/p=1$ up to the E/p at the anode, the total number of ions formed in the avalanche becomes entirely unreasonable, especially for the case of high pressures. It seems therefore necessary to postulate a third region, let us call it S , in which the space charge of the avalanche modifies the electric field in such a way as to limit its size.

This modification is due to the positive ions left behind the avalanche and which, because of their larger mass, are practically stationary compared to the electrons. Their field would be difficult to calculate directly without knowing how much an avalanche spreads as it advances, but it is certainly proportional to their number n . By introducing an empirical constant B , we have

$$E = (2q/r) - Bn. \quad (6)$$

A comparison with the experimental threshold curves leads to the value $B=10^{-10}$ volt/cm \times ions. Because of the fact that the space charge correction contains n , which is an exponential function, the correction has no effect on E until a certain critical value of r and it then has a very large effect.

Equations (5) and (6) can be combined only if the space charge field is small compared to that at the center wire, that is, in the A region. In the S region the effect of the distribution of space charge is too important to allow the simple approximation of Eq. (6). There must be a delicate balance in the S region, the field tending to increase as $1/r$, but on the other hand any increase in field increases the ionization, hence increasing the space charge which decreases the field. It is therefore evident that the field cannot change much, and the simplest assumption is that it remains constant, the ionization being just sufficient to prevent any further increase. This is supported by the agreement with the experimental data.

The shape of the field modified by the space charge of the avalanche computed up to the S region by Eq. (6) and considered constant from r_s , the edge of the space charge region, to r_a is shown in Fig. 4.

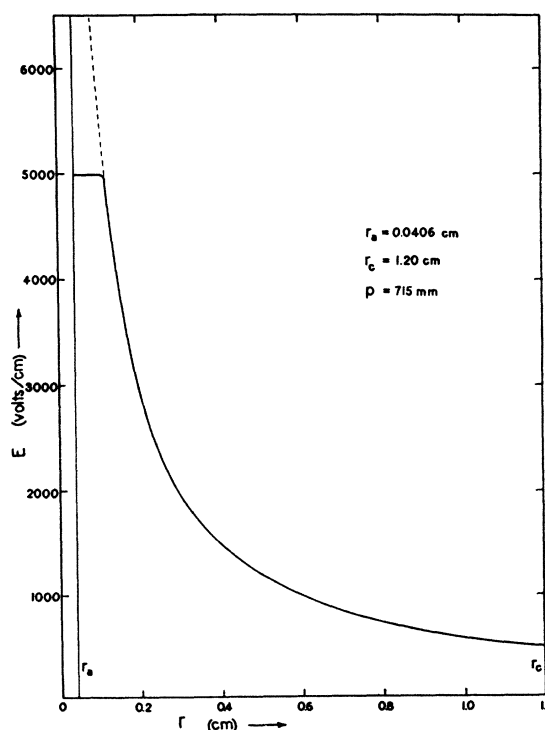


FIG. 4. The solid line shows the field of an avalanche modified by space charge. The dotted line shows how the field would have continued had not space charge had an effect.

**TOTAL NUMBER OF ION PAIRS FORMED
IN INITIAL AVALANCHE**

The total number of ion pairs formed in the initial avalanche in the A region is given directly by Eq. (5).

$$n_a = \exp [2q(u_a - u_c)].$$

The boundary of the S region is defined, somewhat arbitrarily, by

$$\frac{d}{dr} \left(\frac{2q}{r} - Bn \right) = 0.$$

Since $dn = -\alpha n dr$

$$2q/r^2 = Bn\alpha. \quad (7)$$

Using the fact that $E = 2q/r$ and $\alpha = E\eta$ we have

$$r_s = 1/Bn_s\eta_s, \quad (8)$$

where n_s is the number of ions reaching r_s . By solving Eq. (8) by trial and error we can determine r_s , since the number of ion pairs formed from r_c to r_s is given by

$$n_s = \exp [2q(u_s - u_c)]. \quad (9)$$

The total number of ions in the avalanche formed when space charge has an effect is the number formed from r_c to r_s given in Eq. (9), plus the number formed in the constant field from r_s to r_a . The number of ions in the S region is

$$n_a - n_s = n_s \exp [\alpha_s(r_s - r_a)]. \quad (10)$$

By combining Eqs. (9) and (10) and putting it in terms of the variables we have been using in our calculations, the total number of ion pairs formed in the initial avalanche when space

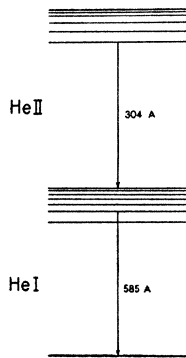


FIG. 5. Schematic energy level diagram of the helium atom.

charge comes into the equation is given by

$$n_a = \exp [2q(u_a - u_c) + 2q\eta_a(1 - r_a/r_s)]. \quad (11)$$

FORM OF THE PHOTOELECTRIC EFFECT

Having determined a satisfactory form for n we now return to our fundamental assumption, the validity of Eq. (1). We must now look for a functional form of γ which will be equal to $1/n$ at breakdown for all cylindrical geometries. If we assume that the secondary electrons are liberated from the cathode through the action of photons, we may set γ equal to the number of photons produced in the gas per ionization, less those absorbed on the way to the cathode, times their photoelectric efficiency. We could designate the corresponding probabilities as ϕ , χ , and ψ . ϕ is then a function of the value of E/p , and therefore of u , in the gas where the ionization occurs as E/p determines the energy of the electronic impacts on the gas atoms. Since three-fourths of the ions are formed in the last two ionization free paths, only the value of E/p at the anode need be considered. χ is a function of the amount of gas which the photon must traverse, which can be represented by pd , the pressure times the distance the photons must travel. ψ depends only on the nature of the photon and of the cathode surface. In general there may be several kinds of photons with different absorption and photoelectric properties, so that γ is in general a sum of terms such as

$$\gamma = \sum_i \phi_i \chi_i \psi_i. \quad (12)$$

The experimental data can be represented by using two such terms, which in general would have the form

$$\gamma = \gamma_I + \gamma_{II} = \exp(-\lambda_1 - \mu_1 pd - \kappa_1 u_a) + \exp(-\lambda_2 - \mu_2 pd - \kappa_2 u_a).$$

Actually, fitting the constants to the data shows that some of these constants are negligible, and the form which appears satisfactory is

$$\gamma = \gamma_I + \gamma_{II} = \exp(-\lambda_1 - \mu pd) + \exp(-\lambda_2 + \kappa u_a), \quad (13)$$

where the constants have the following values:

$$\begin{aligned} \lambda_1 &= 6; & \lambda_2 &= 64; \\ \mu &= 0.25/\text{cm} \times \text{mm Hg}; & \kappa &= 400 \text{ volts/effective} \\ & & & \text{ionization.} \end{aligned}$$

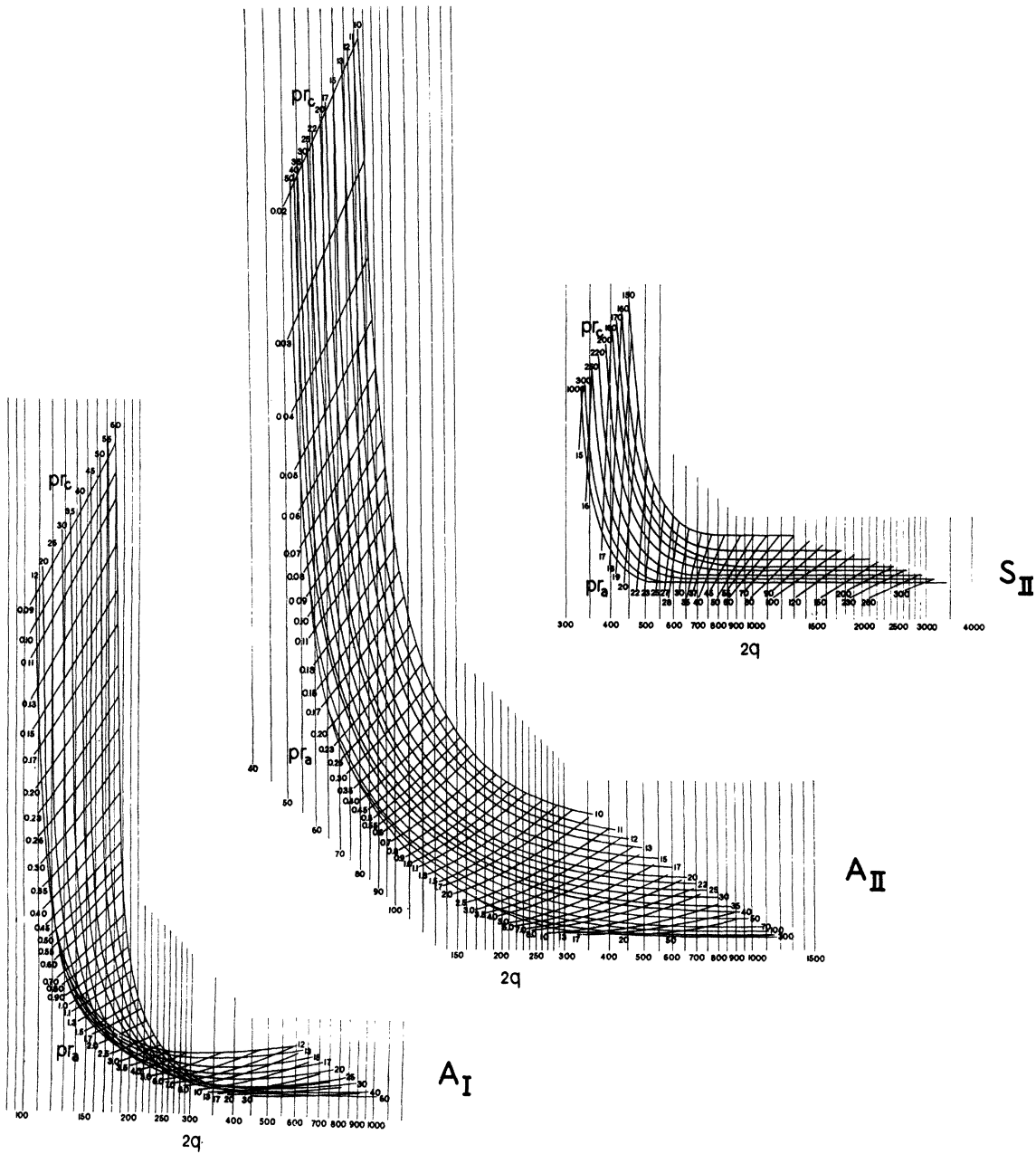


FIG. 6. Theoretical curves for predicting threshold voltages in terms of experimentally observable parameters.

PHYSICAL INTERPRETATION OF THE FORM OF γ

It would appear from the form of Eq. (13) that there are two types of photons involved. The excitation of the first is independent of the energy of impact, but it is strongly absorbed in the gas. The second is more strongly excited by higher energy impacts, but is not absorbed in the gas.

Let us consider for a moment the energy level scheme of the helium atom, a sketch of which is shown in Fig. 5. The most easily excited line in the He I spectrum would be its resonance radiation at 585A. In the process of ionization, the He I spectrum would be fully developed, and therefore the intensity of the lines would be

independent of the mode of excitation and therefore independent of the energy of impact of the electrons in the gas. On the other hand, its outstanding characteristic would be its very high absorption in the helium gas surrounding the discharge, as the photons originating from transitions between excited levels would not be effective photoelectrically. These characteristics are just what is observed in the case of γ_{I} .

The ionization potential of He II is 54 volts. The average voltage drop per ionization in the avalanche in counter discharges lies between 30 and 50 volts. This is the average voltage, of course, so that a fairly large percentage would have energies considerably higher than this. For example, for a mean free path value of 34 volts, 19 percent will go over 57 volts and 14 percent will go over 68 volts. This means that although there is no trouble in exciting He II in the discharge, the spectrum will not be fully developed and therefore the intensity of its lines will depend on its mode of excitation and hence on E/p . On the other hand the 304A resonance radiation of He II would not be expected to be highly absorbed in the normal helium gas of the counter. These are just the characteristics shown by the functional form of γ_{II} .

It seems reasonable, therefore, to adopt the following picture of the photoelectric effects in the initial discharge of a helium counter: In general both the He I and the He II spectrum are excited. Since the resonance radiation of He I is the most copiously produced it will have the dominating effect as long as the pressure in the counter is low enough to allow these photons to reach the cathode. For pressures around 10 mm of Hg, however, the path length in the gas is too long for these photons to reach the cathode, and thereafter the photoelectric effect depends upon the resonance radiation of He II.

THEORETICAL PREDICTION OF THRESHOLD VOLTAGE

Using the breakdown Eq. (1), and the forms of these quantities as given by Eqs. (5), (11), and (13), it would be useful to be able to predict threshold voltages in terms of experimentally convenient parameters. These parameters are p , the pressure of the filling gas; r_a , the radius of the anode; and r_c , the radius of the cathode.

From the point of view of ease in algebraic manipulation four distinct cases will be discussed: A_{I} in which the avalanche is formed in a $1/r$ field and the dominating photoelectric effect is due to the interaction of He I photons and the cathode walls, A_{II} in which the avalanche is formed in $1/r$ field and He II photons are effective, S_{I} in which the avalanche is modified by space charge and He I photons are effective, and S_{II} in which the avalanche is modified by space charge and He II photons are effective.

CASE A_{I}

Treating the A_{I} case first, we can write as Eq. (1)

$$n = \gamma^{-1}.$$

By the use of Eqs. (5) and (13) we may write

$$2q(u_a - u_c) = \lambda_1 + \mu p(r_c - r_a). \quad (14)$$

Let us write Eq. (3) in the form

$$pr_a = 2q/(E_a/p). \quad (15)$$

Equations (14) and (15), together with the plots of Figs. 2 and 3, determine q and η_a in terms of pr_a and pr_c . The breakdown potential follows from q and r_c/r_a by the equation

$$V = 2q \ln(r_c/r_a). \quad (16)$$

The equations are best solved graphically. Equation (15) does not contain pr_c and hence determines a family of curves of $1/\eta_a$ against $2q$, each for an assumed value of pr_c . Eliminating pr_a between Eqs. (14) and (15) we obtain

$$\lambda_1 + \mu pr_c = 2q \left(u_a - u_c + \frac{\mu p}{E_a} \right), \quad (17)$$

and this determines a family of curves of $1/\eta_a$ against $2q$ for assumed values of pr_c . These curves are shown in Fig. 6, plot A_{I} . This plot will allow us to predict threshold voltages for the A_{I} region. We enter the plot with the experimental parameters pr_a and pr_c . The intersection of a pr_a and a pr_c line for a particular case corresponds to a value of $2q$ from which the threshold voltage can be computed by means of Eq. (16).

One of the most noticeable characteristics of this plot is the crossing over of the curves around $2q = 250$. This leads to the prediction that at low pressure for a particular cathode radius, large

values of r_a will have lower threshold voltages than smaller values of r_a , whereas for higher pressures the reverse is true, and the lower the value of r_a , the lower the threshold voltage. This phenomenon has been observed by Haines,⁴ although the precision of the experimental observations in this present work shown in Fig. 1 does not bring out this point.

CASE A_{II}

To obtain a convenient plot from which to predict threshold voltages in the A_{II} region, we

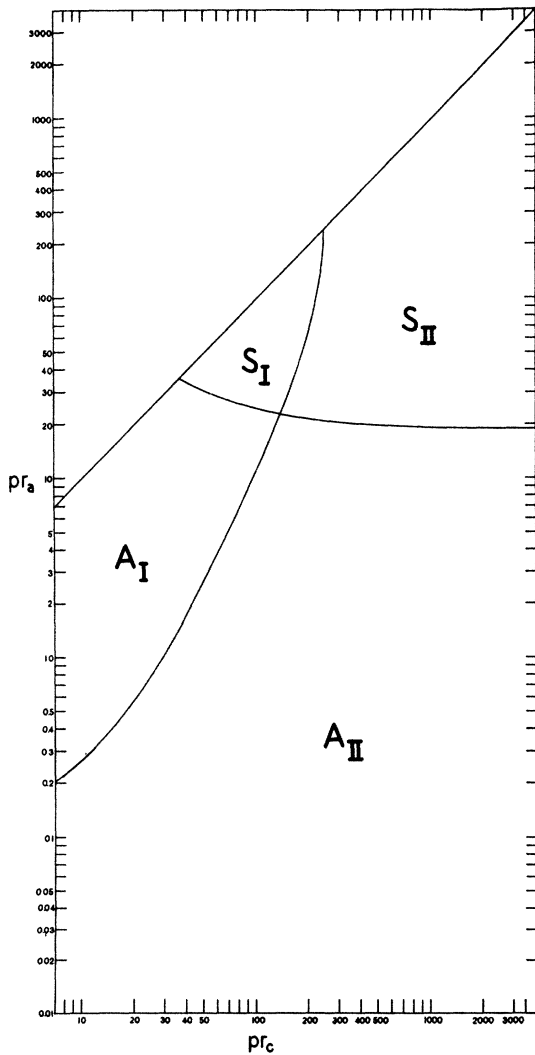


FIG. 7. A theoretical plot showing the regions in which various modes of breakdown take place as a function of experimentally observable parameters.

⁴ C. L. Haines, Rev. Sci. Inst. 7, 411 (1936).

again use Eqs. (5) and (13) to obtain the equation

$$2q(u_a - u_c) = \lambda_2 - \kappa u_a. \tag{18}$$

Here again since we know that

$$E_c/p = 2q/pr_c$$

and u_c is a function of E_c/p , by assuming values of pr_c we can get a family of curves for different values of pr_c by plotting $1/\eta$ as a function of $2q$.

Equation (15) gives us again a method of determining a family of curves for different values of pr_a . The complete plot is shown in plot A_{II} of Fig. 6. The method for using this plot is exactly the same as was described for the A_I plot.

CASE S_{II}

To arrange the equations in a useful form for calculation in the region in which the avalanche is modified by space charge, requires a little more manipulation.

In the S_{II} region we have the expression for n in Eq. (11) and for γ in Eq. (13), so that we may write

$$2q(u_a - u_c) + 2q\eta_a \left(1 - \frac{r_a}{r_s}\right) = \lambda_2 - \kappa u_a, \tag{19}$$

and combining Eqs. (8) and (9), since $u_s = u_a$, we have

$$Br_s\eta_s = \exp [2q(u_c - u_a)]. \tag{20}$$

Equations (15), (19), and (20) determine q , $\eta_s = \eta_a$, and r_s , in terms of pr_a and pr_c . Eliminating pr_c between Eqs. (19) and (20) we obtain

$$2q\eta_a \left(1 - \frac{r_a}{r_s}\right) = \lambda_2 - \kappa u_a + \ln (Br_s\eta_s). \tag{21}$$

Eliminating pr_s between Eqs. (15) and (21) we have

$$2q\eta_a \left(1 - \frac{pr_a E_s}{2q p}\right) = \lambda_2 - \kappa u_a + \ln \left(\frac{B\eta_s}{E_s/p}\right) + \ln \frac{2q}{p}. \tag{22}$$

The last term in this equation turns out, on calculation, to be negligible, so this equation determines the curve of $1/\eta_a$ against $2q$ for assumed values of pr_a .

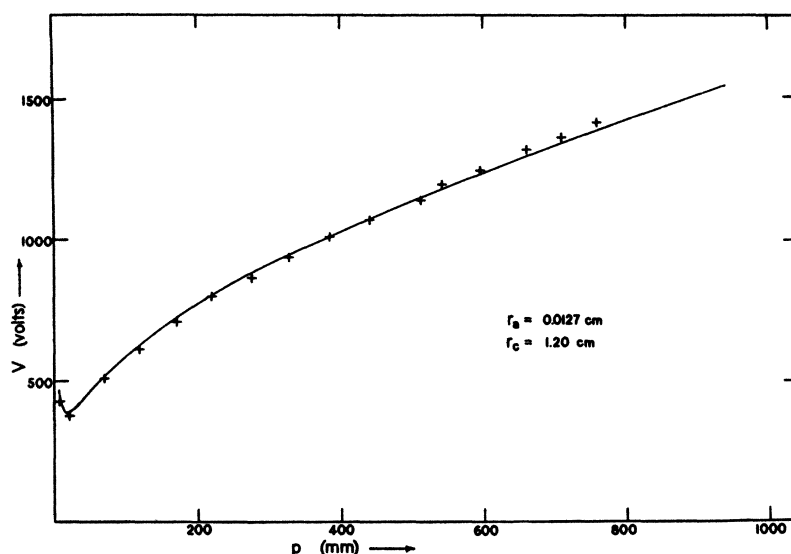


FIG. 8a. Comparison between theoretically predicted threshold voltages (the solid lines) and the experimental points (crosses). A counter falling wholly within the A_{II} region.

Equations (15) and (20) give

$$2q(u_s - u_c) = \ln \left(\frac{E_s/p}{B\eta_s} \right) - \ln \left(\frac{2q}{p} \right), \quad (23)$$

and this equation determines the curve of $1/\eta_a$ against $2q$ for assumed values of pr_c . These two families of curves plotted on each other are shown in Fig. 6, plot S_{II} , and can be used to predict threshold voltages in the S_{II} region in the same manner as was described for the curves in the A_I region.

CASE S_I

In the S_I region, Eq. (19) becomes

$$2q(u_a - u_c) + 2q\eta_a \left(1 - \frac{r_o}{r_s} \right) = \lambda_1 + \mu p(r_c - r_a). \quad (24)$$

Unfortunately in this case, it is not possible to eliminate pr_c between Eqs. (20) and (24), as it appears in the latter both implicitly in u_c and explicitly in μpr_c . In other words, since the function u is expressed only graphically in Fig. 3 and not analytically, no plot of the S_I region has been computed similar to those computed for the other three regions shown in Fig. 6. A fuller discussion of the behavior of a counter operating in this region follows later in this paper.

BOUNDARIES OF THE REGIONS

A brief study of the curves in Fig. 6 will show that for the same values of pr_a and pr_c the different plots will predict different values of $2q$ and therefore different values of threshold voltage. Let us consider the boundaries between the different regions separately. At the boundary between the A_I and the A_{II} or the S_I and the S_{II} regions we have a competition between the He I and the He II radiation as to which will be more effective in producing photoelectrons at the cathode. Whichever is able to do so most readily will have the dominating effect, and therefore whichever plot will predict the lower threshold voltage will be the one to use. On the boundary between the A_I and the S_I region or the A_{II} and the S_{II} region, the question is whether or not the avalanche is modified by space charge. The shape of the field modified by the space charge of the avalanche is shown in Fig. 4. From this plot we can see that physical significance can only be attached to any equation involving this region when the field in the space charge region is equal to or less than the field computed without space charge. This amounts to saying that, for example, Eqs. (20) and (21) do not have physical significance for values of $2q$ below the values of $2q$ from Eqs. (15) and (18). Therefore

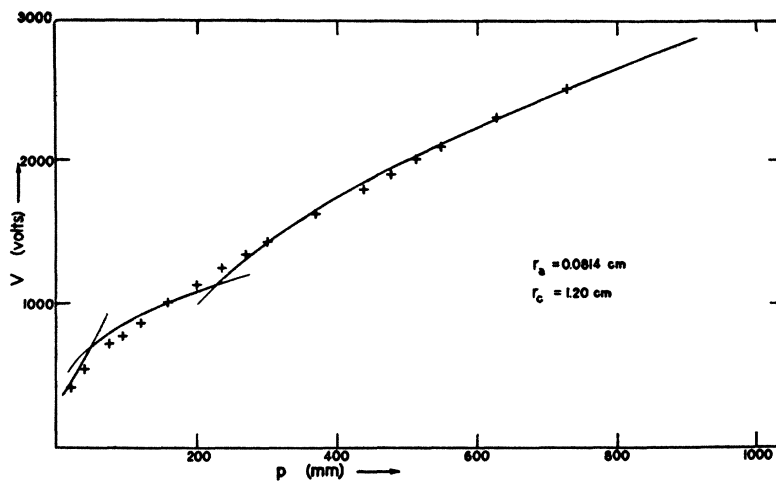


FIG. 8b. A counter starting in the A_I region, passing through the A_{II} region, and ending in the S_{II} region.

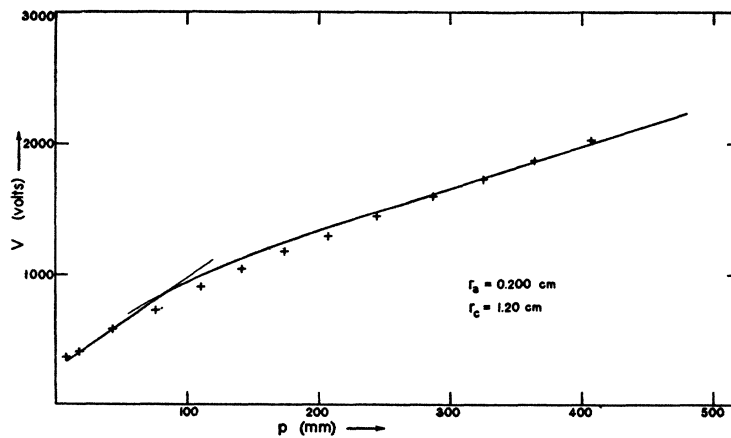


FIG. 8c. A counter passing through the point common to all four regions.

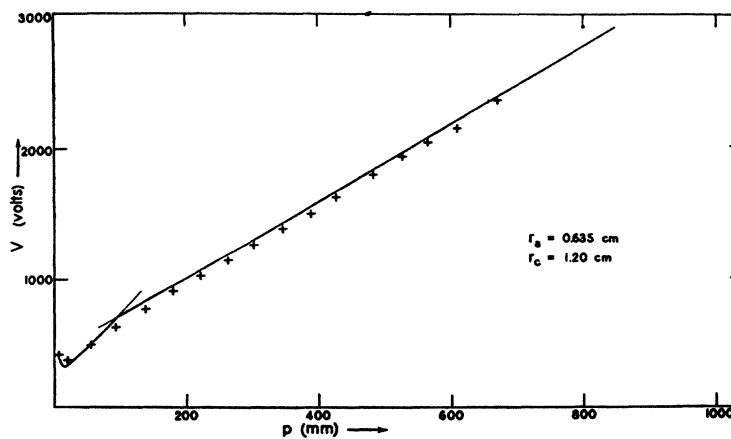


FIG. 8d. A counter starting in the A_I region and ending in the S_{II} region.

the S_{II} plot is only valid when it predicts values of $2q$ and therefore threshold voltages which are equal to or greater than those predicted of the A_{II} plot. This is, of course, what one would expect physically, since it requires more voltage across the electrodes to start a self-maintaining discharge if the field of the avalanche is reduced by space charge than would be the case if space charge were not there.

By knowing the factors which determine the boundaries of the regions in which the different plots are significant, we can compute the boundaries once and for all so that in the actual use of Fig. 6 we can know beforehand which plot we must use.

A plot of the operating regions has been computed and is shown in Fig. 7. One enters this plot with the experimental parameters pr_a and pr_c , and it is immediately evident in what region the counter under these particular conditions is operating. Particular counters, with their fixed values of r_a and r_c , lie in straight lines at 45° on this plot. The upper limiting line drawn on this plot is for the case $r_a=r_c$.

COMPARISON OF THEORY AND EXPERIMENT

The test of any theory is how well it predicts experimentally observed facts. Let us therefore see how well the theoretical curves will fit the experimentally determined values of threshold voltage with changes of pressure for several widely varying cylindrical geometries. This comparison is made in Fig. 8, in which the solid lines are the theoretical curves and the crosses are the experimental points.

Figure 8a is a case in which the counter falls wholly within the A_{II} region, which is generally the case for the so-called Geiger-Müller counters where the center wire is of very small diameter.

Figure 8b is a case in which the counter starts at low pressure in the A_I region, then as the

pressure increases, passes through the A_{II} region, and at high pressure operates wholly within the S_{II} region. No attempt has been made to smooth the theoretical curves as they cross from one region into another. As a matter of fact, they are extended beyond the place where they are significant to emphasize the shapes of the separate theoretical curves.

Figure 8c shows the case for the particular counter which passes through the point common to all the regions. It actually operates in only two regions, A_I and S_{II} .

Figure 8d shows the case of a counter which operates at low pressure in the A_I region, and at high pressures, operates in the S_{II} region. Only the theoretical curves for the A_I and S_{II} regions are given, although it should pass through the S_I region. In this particular example in which $r_c/r_a=1.9$, the S_I region covers a range in pressure of about 50 mm of Hg. The curve would fall above the A_I curve and below the S_{II} at the part of the curve shown in the figure as the junction between the A_I and S_{II} curves. It is both because of the fact that the S_I region is so narrow even when the cathode and anode approach each other in radius, and for the fact that the theoretical predictions are sufficiently good by extrapolating the A_I and S_{II} regions that the much more complicated computation of the S_I region has been omitted.

It can be seen from these examples that it is possible to predict, by means of the present theory, threshold voltages over a wide range of cylindrical geometries, knowing only the experimentally measurable parameters r_a , r_c , and p , and that these predicted curves agree well with the experimental determinations.

In conclusion the author wishes to express his sincere appreciation for the constant help and encouragement of Professor W. P. Allis and Professor Robley D. Evans.